

Topological insulators with perfect vacancy superstructure and possible implications for iron chalcogenide superconductors

Xiao-Yong Feng,¹ Hua Chen,² Chao Cao,¹ and Jianhui Dai^{1,2}

¹*Condensed Matter Group, Department of Physics,
Hangzhou Normal University, Hangzhou 310036, China*

²*Zhejiang Institute of Modern Physics and Department of Physics, Zhejiang University, Hangzhou 310027, China*
(Dated: March 11, 2011)

Motivated by the newly-discovered intercalated iron chalcogenide superconductors, we construct a single orbital tight-binding model for topological insulators on the square lattice with a perfect vacancy superstructure. We find that such lattice structure naturally accommodates a non-vanishing geometry phase associated with the next-nearest-neighbor spin-orbit interaction. By calculating the bulk band structures and the finite stripe edge states, we show that the topological insulator phases can be tuned at certain electron fillings in a wide range of the model parameters. The possible implications of these results for the iron deficient compounds $(A, Tl)_y Fe_{2-x} Se_2$ have been discussed.

PACS numbers: 74.70.Xa, 73.43.Cd, 73.20.-r, 03.65.Vf

Topological insulators (TIs) are a new type of quantum matter which have become evident in electronic systems with appropriate lattice structures and the strong spin-orbit interaction (SOI) [1, 2]. They differ from conventional band insulators with the non-vanishing \mathcal{Z}_2 -odd Kramers states characterized by the gapless counter-propagating excitations on the boundary of materials. Due to the topological nature, such gapless states are robust against weak disorder or interactions. In particular, when these edge states are in proximity to s-wave superconductors, the Majorana fermions could be realized due to the proximity effect [3, 4], and this promises possible applications in spintronics and fault-tolerant topological quantum computation [5, 6].

One of the prototype systems for TIs is the Kane-Mele model which describes tight-binding electrons with the SOI on a two-dimensional honeycomb lattice such as in graphene [7, 8]. However, the SOI turns out to be too small to open a measurable gap in graphene. Zhang and his collaborators predicted the existence of the two-dimensional TI in HgTe/CdTe quantum well structures [9] and it was soon confirmed experimentally by observing the quantized residual conductance caused by edge states [10]. TIs can be also realized in other lattice systems such as in the diamond lattice model which generalizes the 2D honeycomb lattice [11] to three dimensions. As the number of the lattice structures supporting the TI are limited in electronic materials, several schemes are proposed for realizing the topological quantum states in cold-atom systems by taking advantage of the optical lattice in model engineering [18–21].

Meanwhile, three-dimensional TIs have been theoretically predicted [12] and experimentally realized in several realistic materials such as $Bi_{1-x}Sb_x$, Bi_2Se_3 , Bi_2Te_3 , Sb_2Te_3 [13–16], and $TlBiSe_2$ [17]. Recently, the known topological compound Bi_2Te_3 has been shown to exhibit pressure-induced superconductivity with $T_c \sim 3$ K [22]. The real crystal structures in the relevant materials can

be viewed as, more or less, the layered honeycomb and triangle lattices, or the distorted ones like the diamond lattice. It remains a challenge to search for the topological superconductors, or the topological compounds with intrinsic bulk superconductivity at the ambient pressure.

Here we suggest that the TIs, or even the topological superconductors with moderately high transition temperatures at the ambient pressure, could be possibly realized in materials with the crystal structures similar to the ones in the 122-type (I4/m) layered iron chalcogenide superconductors $(A, Tl)_y Fe_{2-x} Se_2$ (with A being the alkali atoms) [23, 24]. One prominent feature of these newly-discovered materials is that there are iron vacancies presumably forming the orthorhombic or tetragonal Fe-vacancy superstructures [24]. Among them, the tetragonal vacancy superstructure (with the Fe-vacancy density 20%) is perfect and most stable, as within each FeSe layer all Fe-atoms are three-coordinated, exhibiting the maximal symmetry with either left- or right-chirality but without breaking the in-plane four-fold rotational invariance, see in Fig. 1(a). This perfect superstructure has been clearly observed by a number of experiments [25–28].

Our suggestion is mainly based on the observation that, though being in the square (or cubic) lattice, the spin-orbit-induced geometric phase (Berry phase) can be naturally protected by the vacancy superstructure. Such lattice can be viewed as a bi-partite lattice with each unit cell containing a minimal square as a block [29]. In Fig. 2 the geometric phase for an electron hopping from the site \mathbf{j} to the next-nearest-neighbor (n.n.n.) site \mathbf{i} with a nearby vacancy is illustrated. Notice that for the intra-block n.n.n. hopping, the associated geometric phases coming from the two permissible paths, both bridged though the Se-atoms in the iron selenides, cancel to each other as in the conventional square lattice. Hence the chiral vacancy ordered lattices (Fig.1(b) or Fig.1(c)) preserve the required symmetry as in the honeycomb or

diamond lattices [7, 8, 11].

In the rest of this paper, we will show that the TI phases can indeed emerge by tuning either band filling or other parameters in a single-orbital tight-binding model defined on the square lattice with the perfect vacancy superstructure (Fig.1(a)). The tight-binding model Hamiltonian we considered is

$$H_t = \sum_{ij} [t_{ij} c_{i\sigma}^\dagger c_{j\sigma} + h.c.]. \quad (1)$$

Where, $c_{i\sigma}^\dagger$ and $c_{i\sigma}$ are the creation and annihilation operators for electrons with spin σ at the site \mathbf{i} . We also assume $t_{ij} = t_1$ or t_2 for the nearest neighbor (n.n.) or the n.n.n. hoppings within a block, and $t_{ij} = t'_1$ or t'_2 for the corresponding hoppings between the two n.n. blocks, and no hopping happens among other sites, see in Fig. 1(b).

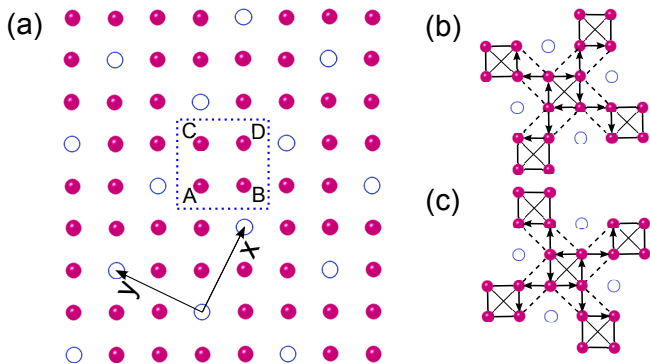


FIG. 1: (a) The perfect vacancy superstructure (clockwise). The open dots represent the Fe-vacancies and one of the block is marked by a dotted square; the x- and y-axes are two directions for the $\sqrt{5} \times \sqrt{5}$ bi-partite block lattice. (b) and (c): The right-handed (clockwise) and left-handed (anti-clockwise) vacancy orderings, respectively. The solid lines are for hoppings and the dashed lines are for SOIs. The arrows indicate the permissible paths for the inter-block SOIs defined by Eq.(2).

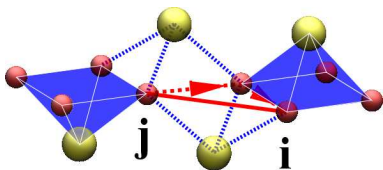


FIG. 2: An electron at the site \mathbf{i} hops to the inter-block n.n.n. site \mathbf{j} in the presence of a nearby vacancy (with the right-handed chirality as shown in Fig.1(b)). This hopping path takes a non-vanishing geometric phase induced by the SOI bridged by the Se-atoms (big yellow) located below or above the Fe-square lattice (small red).

Next, we introduce the SOI for the two n.n.n. sites

$$H_\lambda = i\lambda \sum_{ij} c_{i\sigma}^\dagger \vec{\sigma}_{\sigma\sigma'} \cdot (\vec{e}_i \times \vec{e}_j) c_{j\sigma'}, \quad (2)$$

where $\vec{\sigma} = (\sigma^x, \sigma^y, \sigma^z)$ are the Pauli matrices, \vec{e}_j and \vec{e}_i are unit vectors along the two bonds in series when the electron transfers from \mathbf{j} to \mathbf{i} .

By taking the block as a unit cell and choosing the coordinate directions as shown in Fig.1 [29], we are able to rewrite the total Hamiltonian $H = H_t + H_\lambda$ in the momentum space,

$$H = \sum_{\mathbf{k}\sigma} F_\sigma^\dagger h_\sigma(\mathbf{k}) F_\sigma, \quad (3)$$

where $F_\sigma^\dagger = (c_{A\sigma}^\dagger, c_{B\sigma}^\dagger, c_{C\sigma}^\dagger, c_{D\sigma}^\dagger)$, with $A, B, C,$ and D being the four sites within a block; $h_\uparrow(\mathbf{k})$ is a 4×4 traceless Hermitian matrix with the non-zero matrix elements: $h_{\uparrow 12} = t_1 + (t'_2 + i\lambda)e^{-ik_x}$, $h_{\uparrow 13} = t_1 + (t'_2 - i\lambda)e^{-ik_y}$, $h_{\uparrow 14} = t_2 + t'_1 e^{-ik_y}$, $h_{\uparrow 23} = t_2 + t'_1 e^{ik_x}$, $h_{\uparrow 24} = t_1 + (t'_2 + i\lambda)e^{-ik_y}$, $h_{\uparrow 34} = t_1 + (t'_2 - i\lambda)e^{-ik_x}$; and $h_\downarrow(\mathbf{k}) = h_\uparrow^T(-\mathbf{k})$.

In the absence of the SOI, the bulk band structures were solved in Ref.[29], exhibiting the Dirac-like dispersions near some specific points in the momentum space at the 1/4 or 3/4 electron fillings. Increasing t_2 will generally tune the sub-band gaps, and the mid-band gap may open when the inter-block hopping is (t'_2) sufficiently weak. In order to investigate the topological properties of the system with the SOI, we fix $t_1 = t'_1 = 1$ for simplicity, and consider $t_2 = 0, 0.5, 1.0$, corresponding to zero, moderate, and strong intra-block frustrations, respectively. We find that for each case either the sub-band gaps or the mid-band gap can be opened by tuning λ at certain electron fillings.

The topological nature of the insulating phases can be then investigated by studying the edge states of the strip shaped lattice. The two edges are cut along the x direction with sufficient distance (50 unit cells in the our calculations). The energy spectra are illustrated in Figs.3-5. For $t_2 = 0$, the three gaps among the four bands open gradually with increasing λ , as shown in Figs.3(b,c). Meanwhile, various in-gap states appear within the bulk gaps. Notice that these states are two-fold degenerate for each momentum k_x . We find that a pair of in-gap states cross within the sub-band gap at the 3/4-filling at the time-reversal invariant point $k_x = \pi$. The similar feature is observed at the 1/4-filling at another time-reversal invariant point $k_x = 0$. Meanwhile, two pairs of in-gaps states cross within the mid-band gap at the half-filling near the points $k_x = \pi/2$ and $3\pi/2$, respectively. As we will show later, all these in-gap states in Fig.3 as well as the in-gap states in Figs.4,5 are true edge states.

Of course, the edge states do not necessarily appear when t_2 increases. This is illustrated in the case of $t_2 = 0.5$ in Fig.4(a) ($\lambda = 0.2$), where no edge state appears at the 3/4-filling though the sub-band gap still opens. Notice also that sometimes the edge states can appear at certain electron fillings but no corresponding bulk gap opens. When this happens, the edge states may be coupled to the bulk metallic states upon various scatterings. We find that the condition for the

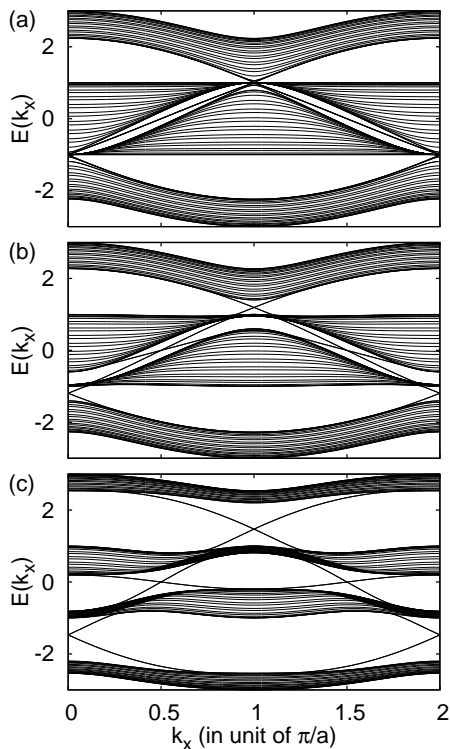


FIG. 3: (a) $\lambda = 0$; (b) $\lambda = 0.2$; (c) $\lambda = 0.6$. In all cases, $t_1 = 1$, $t'_1 = 1$ and $t_2 = t'_2 = 0$.

gapless edge states to appear within the bulk gap is $\Delta = \lambda + t'_2 - t_2 > 0$, as explicitly verified in Fig.4 and Fig.5 for moderate and strong frustration cases respectively. In fact, t'_2 modifies λ and effectively enhances the bulk gap. When $\lambda = t_2 - t'_2$, the Dirac-like dispersion appears at the 3/4 filling as indicated in Fig.4(b) where $t'_2 = 0$, $t_2 = \lambda (= 0.5)$.

The properties of the in-gap or edge states can be further clarified by calculating the amplitudes of the corresponding quasi-particle wavefunctions. The results for the in-gap states (marked by the red and blue points in Fig. 4(c)) are shown in Fig. 6, where the spin orientation for each state is also identified. It is shown that each in-gap state is spatially localized near one of the two edges, while the overlap of the two wave functions is exponentially small. Focusing on one of the edges, the two states with opposite spin z -components propagate along the opposite directions. Hence when the number of such edge state pairs are odd, they are robust against disorders or weak interactions preserving the time reversal symmetry[8]. In our model, such non-trivial TI phases can emerge at the 1/4 or 3/4 electron fillings in a wide parameter region as indicated in Figs. 3(b,c), Fig. 4(c) and Fig. 5(b,c), respectively. The existence of non-trivial TI phases in our model is compatible with the general classification of TIs for systems preserving the time reversal symmetry [30].

Finally, we discuss the possible implications of

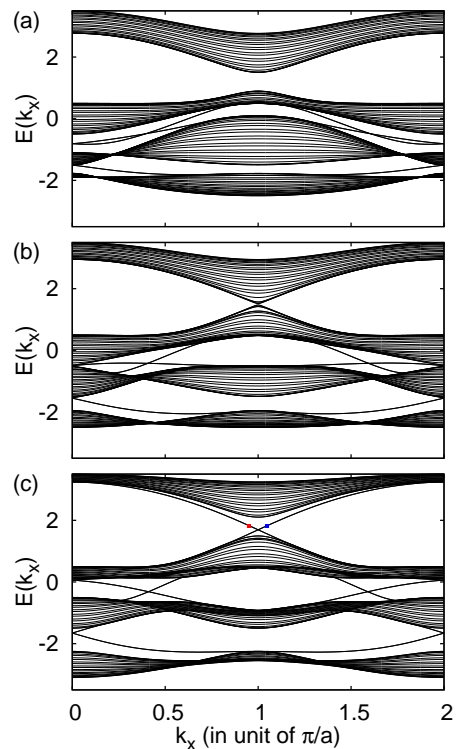


FIG. 4: (a) $\lambda = 0.2$; (b) $\lambda = 0.5$; (c) $\lambda = 0.8$. In all cases, $t_1 = 1$, $t'_1 = 1$, $t_2 = 0.5$ and $t'_2 = 0$.

our results for the newly-discovered iron deficient $(Tl, K)_yFe_{2-x}Se_2$ compounds. These compounds are essentially multi-orbital materials with sizable 3d-4p hybridizations, and the Fe-3d electron correlation may be moderate. Recent first principle calculations find that for $x = 0.4$ a block-spin Néel antiferromagnetic (AFM) ground state can be stabilized in the perfect vacancy superstructure and a band gap $\sim 400 - 500$ meV opens at the Fermi energy when $y = 0.8$, suggesting the Fe^{2+} valence in the charge neutral parent compound [31, 32]. The variation in y just shifts the chemical potential but does not change the block-spin ordering, implying that the perfect vacancy structure is robust. The neutron diffraction experiments suggest that such structure is stable below 550 K or around [26]. Therefore, one of the most important ingredients for our model to host TIs, i.e., the perfect vacancy superstructure which breaks the inversion symmetry by its chirality, could remain *upon various electron or hole dopings* (by tuning y). Another important ingredient, i.e., the SOI, is intrinsic in various chalcogenide-containing materials as in known TIs[13–17]. The inter-block frustration hoppings as well as the SOIs in the intercalated iron chalcogenides are enhanced due the structure distortion [31, 32] (the corresponding Fe-Se-Fe angle is enlarged), so that the condition $\lambda + t'_2 > t_2$ can be satisfied. It is also suggested that the moderate Coulomb interaction can induce the SOI through the mechanism of spontaneous symmetry breaking[33].

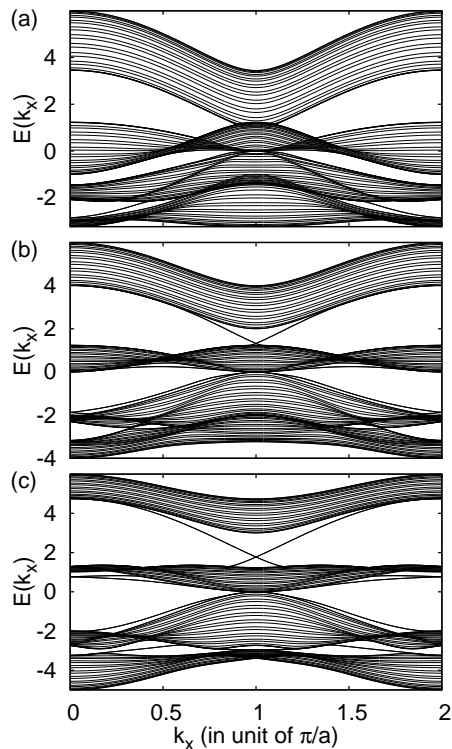


FIG. 5: (a) $\lambda = 0.5$; (b) $\lambda = 1$; (c) $\lambda = 1.5$. In all cases, $t_1 = t'_1 = t_2 = t'_2 = 1$.

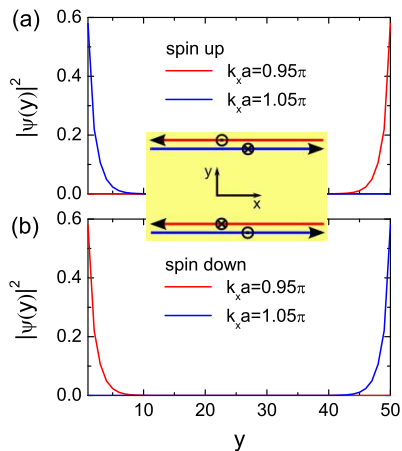


FIG. 6: The wave function amplitudes of the edge states corresponding to the red and blue points indicated in Fig. 4(c). (a) For two spin up states with different momenta; (b) For two spin down states with different momenta.

We can expect that even for relatively strong Coulomb interaction, the TI phases could be transformed to the topological AFM/Mott insulator phases [34]. Lastly, recent experiments have suggested a phase separation [25] or co-existence of the block-spin Néel AFM order and

the superconductivity [26] in $(Tl, K)_yFe_{2-x}Se_2$. Thus it is interesting to see whether the TI phases driven by the ordered vacancies could be in proximity to or co-exist with some kind of superconducting phases in this or other similar compounds. Therefore, this class of materials provides a possible new route of searching for the topological superconductors.

We would like to thank Minghu Fang and Zhuan Xu for helpful discussions. This work was supported by the NSF of China, the NSF of Zhejiang Province, the 973 Project of the MOST and the Fundamental Research Funds for the Central Universities of China (No. 2010QNA3026).

-
- [1] X.L. Qi and S.C. Zhang, *Physics Today* **63**, 33 (2010).
 - [2] M.Z. Hasan and C.L. Kane, *Rev. Mod. Phys.* **82**, 3045 (2010).
 - [3] L. Fu and C.L. Kane, *Phys. Rev. Lett.* **100**, 096407 (2008).
 - [4] F. Wilczek, *Nature Phys.* **5**, 614 (2009).
 - [5] C. Nayak, S.H. Simon, A. Stern, M. Freedman, and S. Das Sarma, *Rev. Mod. Phys.* **80**, 1083 (2008).
 - [6] A.Y. Kitaev, *Ann. Phys.* **303**, 2 (2003).
 - [7] C.L. Kane and E.J. Mele, *Phys. Rev. Lett.* **95**, 146802 (2005).
 - [8] C.L. Kane and E.J. Mele, *Phys. Rev. Lett.* **95**, 226801 (2005).
 - [9] B.A. Bernevig, T.L. Hughes and S.C. Zhang, *Science* **314**, 1757(2006).
 - [10] M. König, *et al.*, *Science* **318**, 766 (2007).
 - [11] L. Fu, C. L. Kane, and E. J. Mele, *Phys. Rev. Lett.* **98**, 106803 (2007).
 - [12] H. Zhang, *et al.*, *Nature Phys.* **5**, 438 (2009).
 - [13] D. Hsieh *et al.*, *Nature* **452**, 970 (2008).
 - [14] Y. Xia, *et al.*, *Nature* **5**, 398 (2008).
 - [15] Y.L. Chen *et al.*, *Science* **325**, 178 (2008).
 - [16] D. Hsieh *et al.*, *Phys. Rev. Lett.* **103**, 146401 (2009).
 - [17] K. Kuroda *et al.*, *Phys. Rev. Lett.* **105**, 146801 (2010).
 - [18] C. Wu, *Phys. Rev. Lett.* **101**, 186807 (2008).
 - [19] L. B. Shao *et al.*, *Phys. Rev. Lett.* **101**, 246810 (2008).
 - [20] T. D. Stanescu, *et al.*, *Phys. Rev. A* **79**, 053639 (2009).
 - [21] M. Kargarian and G.A. Fiete, *Phys. Rev. B* **82**, 085106 (2010).
 - [22] J.L. Zhang *et al.*, *PNAS* **108**, 24 (2011).
 - [23] J. Guo, *et al.*, *Phys. Rev. B* **82**, 180520(R) (2010).
 - [24] M. Fang, *et al.*, arXiv:1012.5236v1 (2010).
 - [25] Z. Wang *et al.*, arXiv:1101.2059 (2011).
 - [26] W. Bao *et al.*, arXiv:1102.0830 (2011).
 - [27] V.Y. Pomjakushin *et al.*, arXiv:1102.3380 (2011).
 - [28] F. Ye *et al.*, arXiv:1102.2882 (2011).
 - [29] H. Chen, C. Cao, and J. Dai, arXiv:1102.4074 (2011).
 - [30] A.P. Schnyder *et al.*, *AIP Conf. Proc.* **1134**, 10 (2009).
 - [31] C. Cao and J. Dai, arXiv:1102.1344 (2011).
 - [32] X.W. Yan, M. Gao, Z.Y. Lu, and T. Xiang, arXiv:1102.2215 (2011).
 - [33] S. Raghu, X.L. Qi, C. Honerkamp, S.C. Zhang, *Phys. Rev. Lett.* **100**, 156401 (2008).
 - [34] D.A. Pesin and L. Balents, *Nature Phys.* **6**, 376 (2010).